MULTI-LEVEL TO 1 BIT TRANSFORMATIONS FOR APPLICATIONS IN DIGITAL-TO-ANALOGUE CONVERTERS USING OVERSAMPLING AND NOISE SHAPING

Conference Paper · November 1988

CITATIONS
4

READS
11

1 author:

Malcolm John Hawksford
University of Essex
235 PUBLICATIONS **1,206** CITATIONS

SEE PROFILE

Proc Institute of Acoustics
Vol 10 : Part 7, 1988
Reproduced Sound 4, Windermere
pp 129-143

MULTI-LEVEL TO 1-BIT TRANSFORMATIONS FOR APPLICATIONS IN DIGITAL-TO-ANALOGUE CONVERTERS USING OVERSAMPLING AND NOISE SHAPING

Dr Malcolm Omar Hawksford

University of Essex, Colchester

0. Introduction

This paper explores an alternative approach to delta-sigma modulation for generating a 1-bit serial code, where a relaxation upon the constraints dictating closed-loop stability enables higher-order loop filters to be used with corresponding gains in target signal-to-noise ratio.

Although the technique has a broader application in communications and digital signal processing, we restrict our investigation to the digital-to-analogue interface required in high performance digital audio systems. Our intention is to devise a digital to analogue converter with greater complexity in the digital domain but with a corresponding simplification in analogue processing. Such a methodology can, in principle, bypass many of the inherent static and dynamic errors found in more conventional converters and also offer a decorrelation of systematic errors resulting from hardware imperfections.

Since 1947 [1-34], there has been extensive investigation of the process of delta modulation. Traditionally, the technique was envisaged as a means of analogue to digital conversion for communication channels and subsequent research spawned numerous methods of enhanced communication efficiency using adaptive control for bit rate reduction. However, the use of adaptive techniques inevitably reflects parametric related distortion with associated deviations from a notionally linear process. In our present application we are not so directed and follow a route that aims to achieve near-linear audio conversion commensurate with 16 to 18 bit resolution. Also, the signal source is already assumed to be digitised and in CD format 44.1 kHz by 16 bit (or similar standard), so our processing is digital except for final analogue reconstruction.

Philips [33] have already investigated this means of conversion and developed a 2nd-order delta-sigma modulator capable of a commendable performance just below that required for the highest performance digital audio systems. Also, earlier papers by Goodman [15] have demonstrated the technique of deltamodulation to pulse code modulation; transformation and Adams [28] has used adaptive deltamodulation as a technique to digitise audio signals.

We commence our study by reviewing the basic processes of deltamodulation and delta-sigma modulation as a prelude to a more general structure to be presented in this paper.

1. Principles of deltamodulation and noise shaping

The deltamodulator shown in Fig.1 is a method of converting a multi-level or continuous signal to a 1-bit serial code such that the serial code, when filtered, forms a close approximation to the input signal.

In general, the coding scheme consists of a recursive loop, where A and B are respectively forward path and feedback path filters, Q an amplitude quantiser usually restricted to two-level quantisation and S a time quantiser to force the output pulse sequence into discrete time slots. Consequently, the input data is quantised in both time and amplitude [20, 21].

It is evident that the input signal must traverse the quantisers Q and S and that Q introduces extreme levels of quantisation noise. However, the process sampling rate greatly exceeds the Nyquist rate

and, together with the networks A, B, the quantisation distortion is noise shaped to locate the majority of system error above the audio baseband (here assumed 20 kHz).

Although the closed-loop response is determined by the combined transfer function AB, the system can be matched to the input spectra. For example, such demarcation of A and B is seen in the classical structures delta modulation [1-4] and delta-sigma modulation [8,9] where Fig.2 illustrates these systems for a first-order loop.

In reviewing the operation of these two classes of deltamodulation, it is important to observe that they are essentially identical, only differing in the point of signal entry, where for a first order loop,

$$AB = \frac{1}{j\omega T} \qquad \ldots 2.1$$

Fig. 2(a) reveals that to reconstruct the input signal with minimal linear distortion, the output pulse sequence $P(n\tau)$ must be shaped by a network (here an integrator) that is identical to that of the feedback transfer function B. This strategy moves against our requirement of generating a two-level serial bit stream. Consequently, we only consider a network derived from Fig.2(b) where A is a noise shaping filter and B = 1.

Research has been directed towards enhancing the coding performance of the basic topology, where if we reject adaptive processes the remaining alternative is to increase the order of the network A by using multiple integrators to enhance noise shaping. For example, two integrators will induce a noise shape proportional to f^2 while a single integrator only achieves f, the implication being that the greater loop gain enforces a lower error level. This is the classical method followed from the earliest papers [1-4].

However, in attempting loop orders >2, limit cycle instability is introduced where the constraint imposed by the 2-level quantiser Q is too restrictive and minimal coding achievement results. The key to controlled stability with high-order loop filters is to extend the quantiser range to multiple levels, together with an effective non-saturating transfer characteristic. Assuming appropriate high-frequency predictive shaping is incorporated, simulation now shows [30,32,34] that controlled loop stability induces intelligent dither and achieves the desired noise shaping characteristic.

In the next Section, we present an extension to this work and introduce a two-stage, delta-sigma modulation type structure using a combination of high-order noise shaping and a multi-level to 1-bit transformer.

2. Two-stage multi-level to 1-bit transformation

The task is to take a digital audio signal M bit by f_{s1} Hz and convert it to a two-level signal at a higher sampling rate, i.e. a signal 1 bit by f_{s3} Hz. In the scheme there are three processes, a sampling rate increase using interpolation followed by a two-stage algorithm to implement the level transformation from M bit to 1 bit. However, in this study we assume perfect interpolation and consider only the two-stage level transformation.

The two-stage converter uses a combination of recursive noise shaping, together with a feedforward, open-loop look-up table. The first stage operates as described in earlier studies

[30,32,34] and combines a noise shaping filter together with a multi-level quantiser, a process that has been shown to achieve a substantial reduction in data word length without incurring a significant noise penalty. This reduction in word length is directly attributable to the added redundancy obtained through an increase in sampling rate. Hence, the output of the first level compaction algorithm is N bit by f_{s2} where $N < M$ and $f_{s1} < f_{s2} < f_{s3}$.

By way of example: f_{s1} = 44.1 kHz, f_{s2} = 11.264 MHz, M = 16 bit, N = 4 bit.

The second stage of the level transformer takes the N bit by f_{s2} signal and using a predetermined look-up table, generates a serial bit sequence 1 bit by f_{s3}. The advantage of this scheme is that the first recursive stage is not constrained by a two-level quantiser which can result in limit cycles, while the non-recursive but truncated look-up table exhibits no stability limitations.

The basic system is shown in Fig.3, where the first stage of level transformation is an optimal noise shaper [24,30,32,34] of general order. Our earlier study [30,34] demonstrated using computer simulation that for a 4th order noise shaper, a typical output sequence spanned a level range of about 16 quanta, yet still achieved a SNR in excess of 100 dB. Consequently, in this example, the look-up table must translate the sample amplitude into a serial bit pattern with a length that can accommodate sixteen levels.

Since there is no one unique code set for implementing this conversion, criteria must be determined for establishing an efficient code table. In the next Section we review the method by which selected pulse patterns can degrade the coding performance and present a selection procedure for choosing enhanced codes for the final open-loop level transformer.

3. Distortion mechanism and optimal code selection in N to 1 bit transformers

The level compaction algorithm of the noise shaper produces a multi-level output signal, where each sample is assumed constant for a period $1/f_{s2}$. The N to 1 bit code conversion takes each level and using a sequence of 1 bit samples, of period $1/f_{s3}$, produces a waveform which, when averaged over $1/f_{s2}$, has the same value as the input sample. This process is demonstrated in Fig.4, where, for illustration, $f_{s3} = 8f_{s2}$ and the input sample is of 4 units.

However, although this example demonstrates how a simple average defined sequence selection operates, it does not describe the inherent dynamic distortion mechanism that is related to the choice of code words.

At this juncture, it is constructive to draw comparisons with uniformly sampled pulse width modulation [35] which seeks a similar goal. In this scheme, a signal sample is converted to a constant amplitude pulse where the width is proportional to sample amplitude; indeed a time-quantised variant of pulse width modulation can form the basis of an open-loop code converter. However, because of signal dependent time dispersion which causes an effective modulation of the pulse spectrum, non-linear distortion is generated. To observe this process, consider the Fourier transform of a unit amplitude rectangular pulse for

$$-\frac{\tau}{2} < t < \frac{\tau}{2},$$

$$F(f) = \tau \, \mathrm{sinc}\left(\frac{\omega\tau}{2}\right) \qquad \ldots (3.1)$$

Equation 3.1 shows that at dc, the average value is proportional to the width τ. However, for $\omega > 0$, the sinc (x) function now distorts the average value by changing the effective gain dynamically with pulse width. This distortion is illustrated in Fig.5 for a range of pulse widths.

In order to minimise distortion in systems that convert an instantaneous sample into a time dispersive structure, the following conditions should be observed:

(i) The average value of each sequence must match exactly the value of the quantised sample.

(ii) The in-audio band amplitude transform of each sequence should closely match.

(iii) The in-audio band phase response of each sequence should be identical.

In general, conditions (i) and (iii) are easily realised for a finite and quantised sequence by choosing pulse patterns that are both even-symmetric about their centre and have bit patterns that average to the sample value being mapped.

However, condition (ii) cannot, in general, be matched exactly due to the limited degrees of freedom defined by a sequence with a finite number of binary elements. Hence, to achieve a minimum distortion it is necessary to select an optimum subset of the available codes which, within the audio band, then exhibit near-identical amplitude transforms when the responses are dc normalised.

Consider a sequence

$$\{d_r\}_{-L/2}^{L/2}$$

of binary pulses of period τ and of length L where for zero phase distortion $d_r = d_{-r}$. The binary elements of the array are represented by logic values 0, 1. However, this symbolic notation maps to actual logic levels as follows:

$$d_r = 1 \rightarrow \hat{D}$$

$$d_r = 0 \rightarrow -\hat{D}$$

where $\hat{D}$ is the maximum sample value to be coded at the output of the noise shaper (e.g. for a 4^{th}-order noise shaper, $\hat{D} = 8$ (typically).

The Fourier transform $F_L(f)$ of this even-symmetric sequence of L elements is then given as,

$$F_L(f)\Big|_{L\ odd} = \tau\left[1 + 2\sum_{r=1}^{L/2} d_r \cos\left(\frac{2\pi\, rf}{f_{s3}}\right)\right]\text{sinc}\left(\frac{\pi f}{f_{s3}}\right) \quad \ldots (3.2)$$

$$F_L(f)\Big|_{L\ even} = \tau\left[2\sum_{r=1}^{L/2} d_r \cos\left(\frac{2\pi(r-0.5)f}{f_{s3}}\right)\right]\text{sinc}\left(\frac{\pi f}{f_{s3}}\right) \quad \ldots (3.3)$$

$$\text{where} \quad \tau = \frac{1}{f_{s3}} \quad \ldots (3.4)$$

The sinc (...) function in equations 3.2, 3.3 arises because the spectrum is calculated using rectangular pulses of period $\tau = 1/f_{s3}$ and amplitude d_r where

$$d_r = \pm \hat{D}$$

These equations are used as the basis of a sifting process to choose the sub-set of codes in a given sequence, length L, which have the closest amplitude responses in the audio band (0 → 20 kHz) and which also meet the desired average value conversion for a sample S_x, where

$$S_x = \frac{1}{L}\sum_{r}^{L} d_r \quad \ldots (3.5)$$

In the next Section, five look-up tables are compared and results presented for a range of noise shaper order $N_S = \{1, 2, 3, 4\}$.

4. SNR computation of translated DSM

To obtain an estimate of SNR performance for the 1-bit converter using noise shaping and look-up table translation, the computational model of Fig.6 was designed. The model consists of two near-identical structures which differ only in their non-linear mechanisms of quantisation and dynamic amplitude response errors. The top channel includes both a quantiser and look-up table while the lower excludes the quantiser and uses a convolution process to generate an amplitude scaled sequence of equally spaced pulses. A low-pass filter (LPF) and difference amplifier then completes the process to produce the error sequence e(n) from which a mean-square value can be computed over a range of input data. By calculating the mean-square value of the input sequence, the SNR is obtained. The advantages of this technique are:

(i) any input excitation can be used

(ii) no problem of FFT analysis over very long data sequences is incurred

(iii) computationally efficient considering the long data sequences

(iv) since actual system is simulated, the results are representative targets for practical hardware.

The paper compares the performance of five selected look-up tables, both to illustrate the technique and to demonstrate the sensitivity to the choice of pulse sequence and its dynamic distortion contribution. In presenting the results two parameters are used to define the noise shaper: R is the oversampling factor and corresponds to the ratio f_{s2}/f_{s1} while N_s is the order of the noise shaper (see ref [30,34]). The final 1-bit serial data rate f_{s3} is defined,

$$f_{s3} = R\,L\,f_{s1} \qquad \ldots (4.1)$$

where, f_{s3}, final output sampling rate

f_{s1}, initial Nyquist sampling rate

R, oversampling ratio

L, look-up table output word length

The results are derived through computer simulation and correspond to the look-up tables presented in tables 1 to 5. In general, SNR calculations are evaluated over a measurement bandwidth 0 - 20 kHz and are plotted for a 20 kHz sine wave input amplitude range of -140 dB to +60 dB where 0 dB corresponds to an amplitude of $1/\sqrt{2}$ volt. For reference, the noise shaper quantiser Q (see Fig. 6) uses uniform quanta spaced with an interval of one volt. In this exercise, the code words are chosen to encode signals to a maximum amplitude of 0 dB, thus saturation is evident for signals in excess of 0 dB.

Comments

Table 1

level	output of look-up table
8	1 1 1 1 1 1 1 1 1 1 1 1 1 1 1 1
7	0 1 1 1 1 1 1 1 1 1 1 1 1 1 1 1
6	0 1 1 1 1 1 1 1 1 1 1 1 1 1 0 1
5	0 1 0 1 1 1 1 1 1 1 1 1 1 1 0 1
4	0 1 0 1 1 1 1 1 1 1 1 1 0 1 0 1
3	0 1 0 1 1 1 1 1 1 1 0 1 0 1 0 1
2	0 1 0 1 0 1 1 1 1 1 0 1 0 1 0 1
1	0 1 0 1 0 1 1 1 0 1 0 1 0 1 0 1
0	0 1 0 1 0 1 0 1 0 1 0 1 0 1 0 1
-1	0 1 0 1 0 1 0 0 0 1 0 1 0 1 0 1
-2	0 1 0 1 0 0 0 0 0 1 0 1 0 1 0 1
-3	0 1 0 1 0 0 0 0 0 0 0 1 0 1 0 1
-4	0 1 0 1 0 0 0 0 0 0 0 0 0 1 0 1
-5	0 1 0 0 0 0 0 0 0 0 0 0 0 1 0 1
-6	0 1 0 0 0 0 0 0 0 0 0 0 0 0 0 1
-7	0 0 0 0 0 0 0 0 0 0 0 0 0 0 0 1
-8	0 0 0 0 0 0 0 0 0 0 0 0 0 0 0 0

A poor performance code conversion where results are shown for R = 200, N_s = {1, 2, 3, 4}. In this case, there are both dynamic amplitude and phase errors as the code is assymetric where the amplitude and phase errors are shown in Fig. 7. In fact, the error in the table is so poor that there is no apparent improvement on total error with increasing noise shaper order. Even so, it would be anticipated that the micro-detail of the distortion between a low-order noise shaper and a non-linear code converter would differ significantly and is an area for further study.

Table 2

level	output of look-up table
8	1 1 1 1 1 1 1 1 1 1 1 1 1 1 1 1 1 1 1 1 1 1 1 1 1 1 1 1 1 1 1 1
7	0 1 1 1 1 1 1 1 1 1 1 1 1 1 1 1 1 1 1 1 1 1 1 1 1 1 1 1 1 1 1 0
6	0 1 1 1 1 1 1 1 1 1 1 1 1 1 0 1 1 0 1 1 1 1 1 1 1 1 1 1 1 1 1 0
5	0 1 0 1 1 1 1 1 1 1 1 1 1 1 0 1 1 0 1 1 1 1 1 1 1 1 1 1 1 0 1 0
4	0 1 0 1 1 1 1 1 1 1 1 1 0 1 0 1 1 0 1 0 1 1 1 1 1 1 1 1 1 0 1 0
3	0 1 0 1 1 1 1 1 1 1 0 1 0 1 0 1 1 0 1 0 1 0 1 1 1 1 1 1 1 0 1 0
2	0 1 0 1 0 1 1 1 1 1 0 1 0 1 0 1 1 0 1 0 1 0 1 1 1 1 1 0 1 0 1 0
1	0 1 0 1 0 1 1 1 0 1 0 1 0 1 0 1 1 0 1 0 1 0 1 0 1 1 1 0 1 0 1 0
0	0 1 0 1 0 1 0 1 0 1 0 1 0 1 0 1 1 0 1 0 1 0 1 0 1 0 1 0 1 0 1 0
-1	1 0 1 0 1 0 0 0 1 0 1 0 1 0 1 0 0 1 0 1 0 1 0 1 0 0 0 1 0 1 0 1
-2	1 0 1 0 1 0 0 0 0 0 1 0 1 0 1 0 0 1 0 1 0 1 0 0 0 0 0 1 0 1 0 1
-3	1 0 1 0 0 0 0 0 0 0 1 0 1 0 1 0 0 1 0 1 0 1 0 0 0 0 0 0 0 1 0 1
-4	1 0 1 0 0 0 0 0 0 0 0 0 1 0 1 0 0 1 0 1 0 0 0 0 0 0 0 0 1 0 1
-5	1 0 1 0 0 0 0 0 0 0 0 0 0 0 1 0 0 1 0 0 0 0 0 0 0 0 0 0 1 0 1
-6	1 0 0 0 0 0 0 0 0 0 0 0 0 0 1 0 0 1 0 0 0 0 0 0 0 0 0 0 0 0 1
-7	1 0 0 0 0 0 0 0 0 0 0 0 0 0 0 0 0 0 0 0 0 0 0 0 0 0 0 0 0 0 1
-8	0 0 0 0 0 0 0 0 0 0 0 0 0 0 0 0 0 0 0 0 0 0 0 0 0 0 0 0 0 0 0

In table 2 the length of code is doubled, which allows for a symmetric pattern that eliminates phase error. In this scheme a pattern generator was used which progressively increased sequences of alternating 1 0 1 0 s, although the patterns were not selected for minimum dynamic errors. The resulting SNR for R = 200, N_s = {1, 2, 3, 4} is shown in Fig. 8 where substantial improvement is demonstrated, particularly for N = 1 where few codes are exercised. However, for N_s = {3, 4} this is not the case where dynamic distortion now causes the curves to merge.

Table 3

level	output of look-up table
8	1 1 1 1 1 1 1 1 1 1 1 1 1 1 1 1 1 1 1 1 1 1 1 1 1 1 1 1 1 1 1 1
7	1 1 1 1 1 1 0 1 1 1 1 1 1 1 1 1 1 1 1 1 1 1 1 1 1 0 1 1 1 1 1 1
6	1 1 1 0 1 1 1 1 1 1 1 1 0 1 1 1 1 1 1 0 1 1 1 1 1 1 1 1 0 1 1 1
5	1 1 1 0 1 1 1 1 0 0 1 1 1 1 1 1 1 1 1 1 1 1 0 0 1 1 1 1 0 1 1 1
4	1 0 1 1 1 1 1 0 0 1 1 1 1 1 0 1 1 0 1 1 1 1 1 1 0 0 1 1 1 1 1 0 1
3	1 1 1 1 0 0 0 0 1 1 1 0 1 1 1 1 1 1 1 1 0 1 1 1 0 0 0 0 1 1 1 1
2	1 0 1 0 1 1 0 1 1 0 1 1 0 1 1 0 0 1 1 0 1 1 0 1 1 0 1 1 0 1 0 1
1	1 1 1 0 0 0 0 1 0 1 0 0 1 1 1 1 1 1 1 1 0 0 1 0 1 0 0 0 0 1 1 1
0	0 1 1 0 1 0 0 1 1 0 0 1 0 1 1 0 0 1 1 0 1 0 0 1 1 0 0 1 0 1 1 0
-1	0 0 0 1 1 1 1 0 1 0 1 1 0 0 0 0 0 0 0 0 1 1 0 1 0 1 1 1 1 0 0 0
-2	0 1 0 1 0 0 1 0 0 1 0 0 1 0 0 1 1 0 0 1 0 0 1 0 0 1 0 0 1 0 1 0
-3	0 0 0 0 1 1 1 1 0 0 0 1 0 0 0 0 0 0 0 0 1 0 0 0 1 1 1 1 0 0 0 0
-4	0 1 0 0 0 0 0 1 1 0 0 0 0 0 1 0 0 1 0 0 0 0 0 1 1 0 0 0 0 0 1 0
-5	0 0 0 1 0 0 0 0 1 1 0 0 0 0 0 0 0 0 0 0 0 1 1 0 0 0 0 1 0 0 0
-6	0 0 0 1 0 0 0 0 0 0 0 0 0 1 0 0 0 0 0 0 1 0 0 0 0 0 0 0 0 1 0 0 0
-7	0 0 0 0 0 0 1 0 0 0 0 0 0 0 0 0 0 0 0 0 0 0 0 0 0 0 1 0 0 0 0 0 0
-8	0 0 0 0 0 0 0 0 0 0 0 0 0 0 0 0 0 0 0 0 0 0 0 0 0 0 0 0 0 0 0 0

Again a 16 bit sequence is chosen, but a computer search has been performed to select the set of codes with the smallest difference within the audio band. In Fig. 9 the spectra of code words in look-up table 3 is shown, while in Fig. 10 the corresponding SNR predictors are given for R = 200, $N_s = \{1,2,3,4\}$. This table achieved results within about 3 dB (input = 0 dB) of the noise shaper with multi-level conversion (16 levels) [34] and thus indicates minimal distortion over the basic noise shaper.

Table 4

levels	output of look-up table
7.5	1 1 1 1 1 1 1 1 1 1 1 1 1 1 1
6.5	1 1 1 1 1 1 1 0 1 1 1 1 1 1 1
5.5	1 1 1 0 1 1 1 1 1 1 1 0 1 1 1
4.5	1 1 0 1 1 1 1 0 1 1 1 1 0 1 1
3.5	1 0 1 1 1 1 0 1 0 1 1 1 1 0 1
2.5	1 0 1 1 0 1 1 0 1 1 0 1 1 0 1
1.5	1 0 1 0 1 0 1 1 1 0 1 0 1 0 1
0.5	1 0 0 1 1 0 1 0 1 0 1 1 0 0 1
-0.5	0 1 1 0 0 1 0 1 0 1 0 0 1 1 0
-1.5	0 1 0 1 0 1 0 0 0 1 0 1 0 1 0
-2.5	0 1 0 0 1 0 0 1 0 0 1 0 0 1 0
-3.5	0 1 0 0 0 0 1 0 1 0 0 0 0 1 0
-4.5	0 0 1 0 0 0 0 1 0 0 0 0 1 0 0
-5.5	0 0 0 1 0 0 0 0 0 0 0 1 0 0 0
-6.5	0 0 0 0 0 0 0 1 0 0 0 0 0 0 0
-7.5	0 0 0 0 0 0 0 0 0 0 0 0 0 0 0

A reduction from 32 bit to 15 bit is achieved by using a mid-riser quantiser instead of a mid-tread quantiser (see Q in Fig. 6), where input amplitudes for $N_s = 4$ now range from -7.5 ... - 0.5, 0.5 ... +7.5, i.e. there is one less level as zero is excluded. However, in this table not all code words are optimal, where for example the codes 6.5 and -6.5 are not interchangeable with alternative patterns and, in fact, contribute significant error. In Fig. 11(a), the spectral plots of those code words are shown (0 - 60 kHz), together with the corresponding SNR plots in Fig. 11(b). The simulations suggest that for $N_s = 4$ as much as 30 dB of SNR is lost compared with the 16-level digital to analogue converter.

Table 5

level	O\P of look-up table
7.5	1 1 1 1 0 1 1 1 1 1 1 1 1 1 0 1 1 1 1
6.5	1 1 0 1 1 1 1 1 1 0 1 1 1 1 1 1 0 1 1
5.5	1 1 1 0 0 1 1 1 1 1 1 1 1 1 0 0 1 1 1
4.5	1 1 0 1 0 1 1 1 1 0 1 1 1 1 0 1 0 1 1
3.5	1 0 1 1 0 1 1 1 0 1 0 1 1 1 0 1 1 0 1
2.5	1 0 1 1 0 0 1 1 1 0 1 1 1 0 0 1 1 0 1
1.5	1 0 1 0 1 0 1 0 1 1 1 0 1 0 1 0 1 0 1
0.5	0 1 0 1 1 1 1 0 0 0 0 0 1 1 1 1 0 1 0
-0.5	1 0 1 0 0 0 0 1 1 1 1 1 0 0 0 0 1 0 1
-1.5	0 1 0 1 0 1 0 1 0 0 0 1 0 1 0 1 0 1 0
-2.5	0 1 0 0 1 1 0 0 0 1 0 0 0 1 1 0 0 1 0
-3.5	0 1 0 0 1 0 0 0 1 0 1 0 0 0 1 0 0 1 0
-4.5	0 0 1 0 1 0 0 0 0 1 0 0 0 0 1 0 1 0 0
-5.5	0 0 0 1 1 0 0 0 0 0 0 0 0 0 1 1 0 0 0
-6.5	0 0 1 0 0 0 0 0 0 1 0 0 0 0 0 0 1 0 0
-7.5	0 0 0 0 1 0 0 0 0 0 0 0 0 0 0 1 0 0 0

A modified table to 4 suggested by Li Mu (see Acknowledgement) adds four bits to the patterns of table 4 and thus gives a greater code choice. The spectral plots of table 5 are shown in Fig. 12, while in Fig. 13, four SNR plots for R = {25, 50, 100, 200} are illustrated. The simulations suggest that for $N_S = 4$, table 5 produces a 7 dB degradation in SNR compared with table 3, but offers the advantage of a lower bit rate.

5. Conclusion

An alternative algorithm to delta-sigma modulation has been presented as a means of multi-level to one bit transformation for use in digital to analogue conversion applications. The technique circumvents the usual limit cycle restriction of high-order delta-sigma modulation and readily enables a noise shaping filter with an order > 2 to be used. The key to the process was the combination of a high-order, multi-level noise shaper in association with an open-loop, look-up table.

Computer simulation evaluated five look-up tables and revealed the significance of selecting codes with low dynamic distortion. Symmetrical codes were shown to eliminate phase-error distortion, while computer selection sifted codes for similar amplitude responses within the audio band to produce a significant reduction in distortion.

In practice, best performance was achieved using a 32 bit code in conjunction with a 4^{th}-order noise shaper. However, a code using only 19 bits was also demonstrated to yield an acceptable result with the advantage of a lower bit rate.

An important attribute of a coding scheme with an order > 2 is the ability to code low-level signals without the modulation artefacts common to delta-sigma modulation. The SNR curves of a 4^{th}-order noise shaper with look-up table are significantly smoother with changes in level compared with those of a 2nd-order delta-sigma modulator.

In compiling these results, examples have been selected only for a limited range of order, oversampling ratio and conversion code. Further study suggests that, for a given pulse rate, there is an optimal balance between noise filter order and oversampling ratio to maximise the SNR and that for high oversampling ratios, the two-stage system significantly outperforms delta-sigma modulation (using second-order filters).

In limiting the length of code word, the system exhibits amplitude saturation as evident from the high-level SNR plots. However, it should be observed that saturation is not primarily a function of the noise shaper (though this must have a limit), but of the look-up table, where if an input address exceeds the limits ± 8 (for $N_s = 4$), amplitude clipping distortion results. The longer codes can, of course, be coded to accommodate a wider amplitude range.

The application for this conversion process is targeted at high performance digital audio where a wide dynamic range is encountered and where accurate coding into the noise floor is required. Also, in such schemes the relaxation of analogue hardware requirements should be welcome, where the digital-to-analogue converter reduces to a one bit high-speed gate and analogue recovery is achievable using basic passive filtration.

Although certain conversion codes significantly degrade performance, the error contribution is somewhat different to that of a 2nd-order delta-sigma modulation and due to the effective intelligent dither [34] of a noise shaper, should generate only benign noise. Also, a process where the boundaries between noise and structured distortion are blurred, the concepts of Fuzzy set theory may well prove applicable and relate to the earlier proposal of a Fuzzy Distortion [27]. Hence, future research should attempt to gain a greater insight into these distortion processes and also attempt a unification with high-order pulse width modulation which is also applicable to the two-stage transformer as being a special case of code conversion.

6. Acknowledgement

I wish to acknowledge the work of Mr Li Mu, a Telecommunications Systems M.Sc. student at Essex University from 1987-88, whose project work enabled the generation of results presented in this paper and who also proposed Table 5.

7. References

1. Deloraine, E.M., Van Mierlos and Derjavitch, "Methods et systeme de transmission par impulsions", French Patent 932.140, 1947/48.

2. French Patent specification: No.987.238, 23rd May 1949

3. Schouten, J.F., de Jager, F. and Greefkes, J.A., "Deltamodulation, a new modulation system for telecommunications", *Philips Tech. Tidjdschr.* , **13**, p.249, September 1951 (in Dutch); *Philips Tech. Rev.* , **13**, p.237, March 1952

4. de Jager, "Deltamodulation, a method of PCM transmission using 1-unit code", *Philips. Res. Rep. 7,* pp.442-466, 1952

5. Van de Weg, H, "Quantising noise of a single-integration deltamodulation system with an N-digit code", *Philips Res. Rep. 8,* p.367, 1953

6. Nakamara, Y. and Kaneko, H., "Deltamodulation encoder", *NEC Research and Development,* **No.1,** 621.376.56:621.382, p.45, October 1960

7. Lender, A. and Kazuch, M., "Single-bit deltamodulation system", *Electronics,* p.125, November 1961

8. Inose, H., Yasuda, Y. and Murakami, J., "A telemetering system by code modulation - $\Delta\Sigma$ modulation", *IRE Trans.,* **PGSET 8,** p.204, September 1962

9. Inose, H. and Yasuda, Y., "A unity bit coding method by negative feedback", *Proc. IEEE,* **Vol.51,** p.1524, November 1963

10. Halijak, A. and Tripp, J.S., "A deterministic study of deltamodulation", *IRE Int. Conv. Rec.,* **pt. 8,** p.247, 1963

11. O'Neal, J.B., "Deltamodulation quantisation noise analytical and computer simulation results for Gaussian and television input signals", *BSTJ,* **45,** No.1, p.232, January 1966

12. O'Neal, J.B., "A bound on signal-to-quantisation noise ratios for digital encoding systems", *Proc. IEEE, Vol.55,* No.3., p.287, March 1967

13. Protonotarios, E.N., "Slope overload noise in differential pulse code modulation", *BSTJ,* **46,** No.9., p.2119, November 1967

14. Greefkes, J.A. and de Jager, F., "Continuous deltamodulation", *Philips Res. Report,* p.233, 1968

15. Goodman, D.J., "The application of deltamodulation to analog-to-PCM-encoding", *BSTJ*, **Vol.48,** No.2, p.321, February 1969

16. Goodman, D.J., "Delta-modulation granular quantising noise", *BSTJ*, **48,** pt. 1, p.1197, May/June 1969

17. Iwersen, J.E., "Calculated quantisation noise of single-integration deltamodulation coders", *BSTJ*, **Vol.48,** No.7., p.2359, September 1969

18. Laane, R.R., "Measured quantisation noise spectrum for single-integration, deltamodulation coders", *BSTJ*, **Vol.49,** No.2., p.159, February 1970

19. Dalton, C.J., "Deltamodulation for sound distribution: A general survey", *BBC Res. Report,* **Report No. 1971/12,** UDC 621.376.5

20. Flood, J.E. and Hawksford, M.J., "Exact model for deltamodulation processes", *Proc. IEE,* **Vol.118,** p.115, 1971

21. Hawksford, M.J., "Unified theory of digital modulation", *Proc. IEE,* **Vol.121/2,** pp.109-115, February 1974

22. Hawksford, M.J., "Deltamodulation coder using a parallel realisation", *IERE Conference Proc.*, **37,** pp.547-557, September 1977

23. Steele, R., *Deltamodulation sytems*, Pentech Press (London), ISBN 07273 0401 1, 1975

24. Tewksbury, S.K., Hallock, R.W., "Oversampled linear predictive and noise-shaping coders of order N>1", *IEEE Trans. on Circuits and Systems,* **Vol. CAS 25/7,** July 1978

25. Candy, J.C. and Benjamin , O.J., "The structure of quantisation noise from sigma-delta modulation", *IEEE Trans. on Communications,* **Vol.COM-29/9,** September 1981

26. Goadhart, D., van de Plassche, R.J. and Stikvoort, E.F., "Digital-to-analogue conversion in playing compact disc", *Philips Tech. Rev.*, **40,** No.6, 174-179, 1982

27. Hawksford, M.J., "Fuzzy distortion in analog amplifiers: A limit to information transmission?", *JAES,* **Vol.31,** No.10, pp.745-754, October 1983

28. Adams, R.W., "Companded predictive deltamodulation: A low cost conversion technique for digital recording", *JAES,* **Vol.32,** No.9, pp.659-672, September 1984

29. Candy, J.C., "A use of double integration in sigma deltamodulation", *IEEE Trans. Comm.,* **COM-33,** pp.249-258, March 1985

30. Hawksford, M.J., "N^{th}-order recursive sigma-ADC machinery at the analogue-digital gateway", 78th AES Convention, *Preprint 2248 (A-15),* May 1985

31. Adams, R.W., "Design and implementation of an audio 18-bit analogue-to-digital converter using oversmapling techniques", *JAES,* **Vol.34,** No.3., pp.153-166, March 1986

15. Goodman, D.J., "The application of deltamodulation to analog-to-PCM-encoding", *BSTJ*, **Vol.48,** No.2, p.321, February 1969

16. Goodman, D.J., "Delta-modulation granular quantising noise", *BSTJ*, **48,** pt. 1, p.1197, May/June 1969

17. Iwersen, J.E., "Calculated quantisation noise of single-integration deltamodulation coders", *BSTJ*, **Vol.48,** No.7., p.2359, September 1969

18. Laane, R.R., "Measured quantisation noise spectrum for single-integration, deltamodulation coders", *BSTJ*, **Vol.49,** No.2., p.159, February 1970

19. Dalton, C.J., "Deltamodulation for sound distribution: A general survey", *BBC Res. Report,* **Report No. 1971/12,** UDC 621.376.5

20. Flood, J.E. and Hawksford, M.J., "Exact model for deltamodulation processes", *Proc. IEE,* **Vol.118,** p.115, 1971

21. Hawksford, M.J., "Unified theory of digital modulation", *Proc. IEE,* **Vol.121/2,** pp.109-115, February 1974

22. Hawksford, M.J., "Deltamodulation coder using a parallel realisation", *IERE Conference Proc.*, **37,** pp.547-557, September 1977

23. Steele, R., *Deltamodulation sytems*, Pentech Press (London), ISBN 07273 0401 1, 1975

24. Tewksbury, S.K., Hallock, R.W., "Oversampled linear predictive and noise-shaping coders of order N>1", *IEEE Trans. on Circuits and Systems,* **Vol. CAS 25/7,** July 1978

25. Candy, J.C. and Benjamin , O.J., "The structure of quantisation noise from sigma-delta modulation", *IEEE Trans. on Communications,* **Vol.COM-29/9,** September 1981

26. Goadhart, D., van de Plassche, R.J. and Stikvoort, E.F., "Digital-to-analogue conversion in playing compact disc", *Philips Tech. Rev.*, **40,** No.6, 174-179, 1982

27. Hawksford, M.J., "Fuzzy distortion in analog amplifiers: A limit to information transmission?", *JAES,* **Vol.31,** No.10, pp.745-754, October 1983

28. Adams, R.W., "Companded predictive deltamodulation: A low cost conversion technique for digital recording", *JAES,* **Vol.32,** No.9, pp.659-672, September 1984

29. Candy, J.C., "A use of double integration in sigma deltamodulation", *IEEE Trans. Comm.,* **COM-33,** pp.249-258, March 1985

30. Hawksford, M.J., "N^{th}-order recursive sigma-ADC machinery at the analogue-digital gateway", 78th AES Convention, *Preprint 2248 (A-15),* May 1985

31. Adams, R.W., "Design and implementation of an audio 18-bit analogue-to-digital converter using oversmapling techniques", *JAES,* **Vol.34,** No.3., pp.153-166, March 1986

32. Stritek, P., "Prospective techniques for improved signal-to-noise ratio in digital audio conversion sytems", 82nd Convention of JAES, *Preprint 2477 (M-2)*, March 1987

33. Naus, P.J., Dijkmans, E.C., Stikvoort, E.F., McKnight, A.J., Holland, D.J. and Bradinal, W., "A CMOS stereo 16-bit D/A converter for digital audio", *IEEE J.*, Solid State Circuits, **SC-22**, No.3, June 1987

34. Hawksford, M.J., "Oversampling and noise shaping for digital to analogue conversion", Institute of Acoustics, *Reproduced Sound 3*, pp.151-175, 1987

35. Sandler, M., "Techniques for digital power amplification", Institute of Acoustics, *Reproduced Sound 3*, pp.177-186, 1987

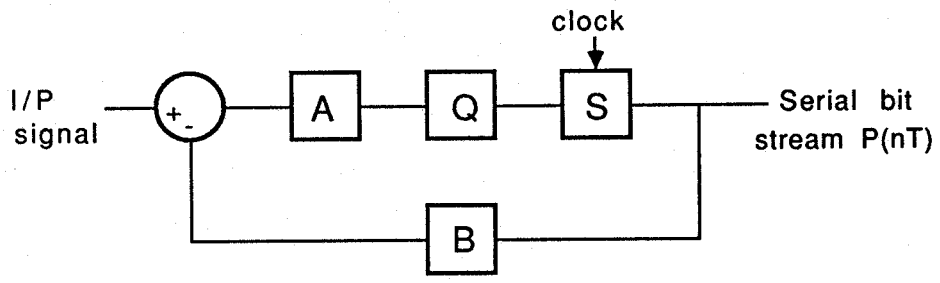

Fig. 1 General delta-modulator coder.

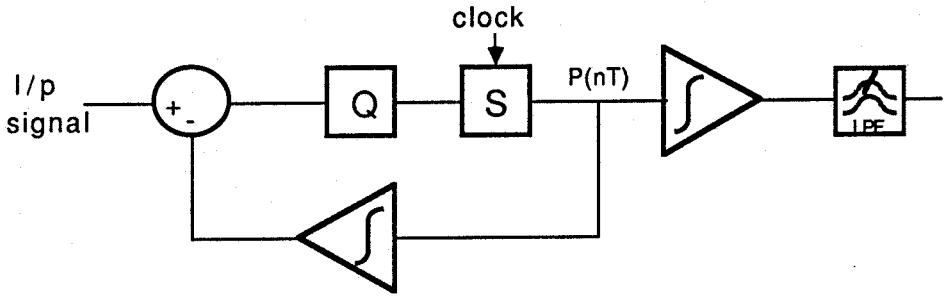

(a) Deltamodulation.

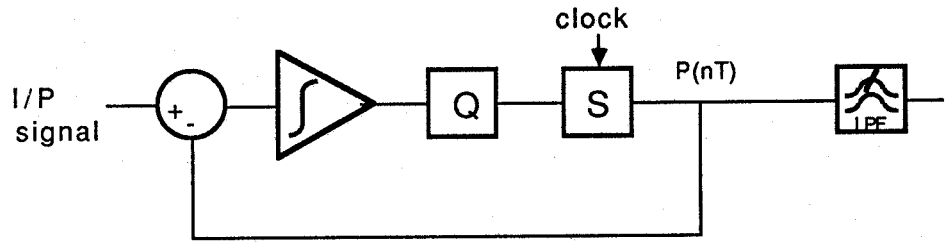

(b) Delta-modulation.

Fig. 2 Classical delta / delta-sigma modulation.

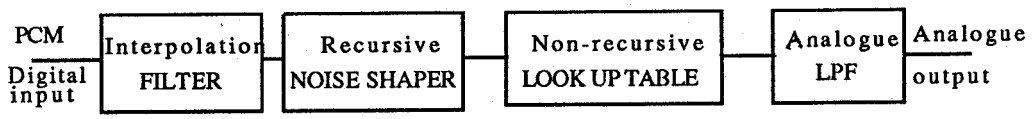

Fig.3a Basic 2-stage recursive/non-recursive noise shaping pcm to 1-bit DAC.

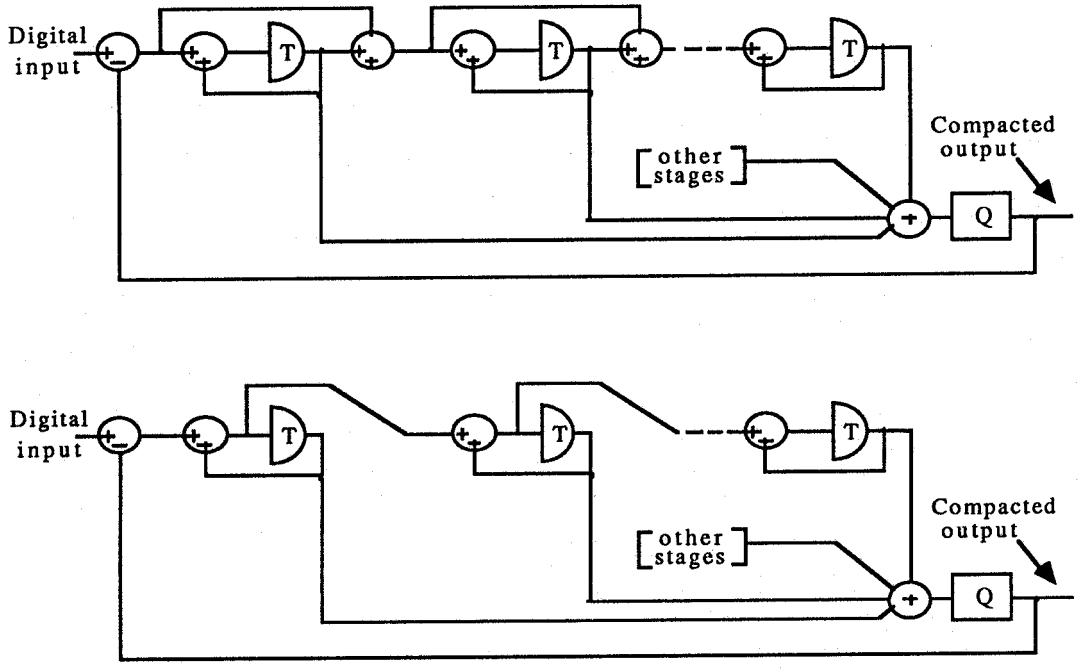

Fig 3b Recursive noise shaper (feedforward paths and equivalent illustrated).

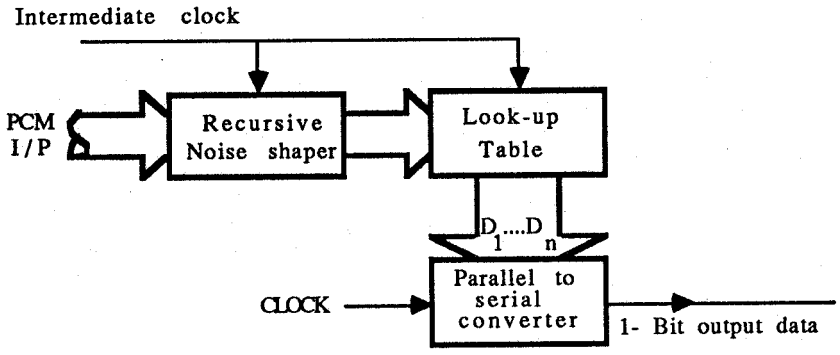

Fig.3c Basic m-Bit to 1-Bit transformer.

Fig.3 M-bit to 1-bit transformer using recursive and nonrecursive noise shaping

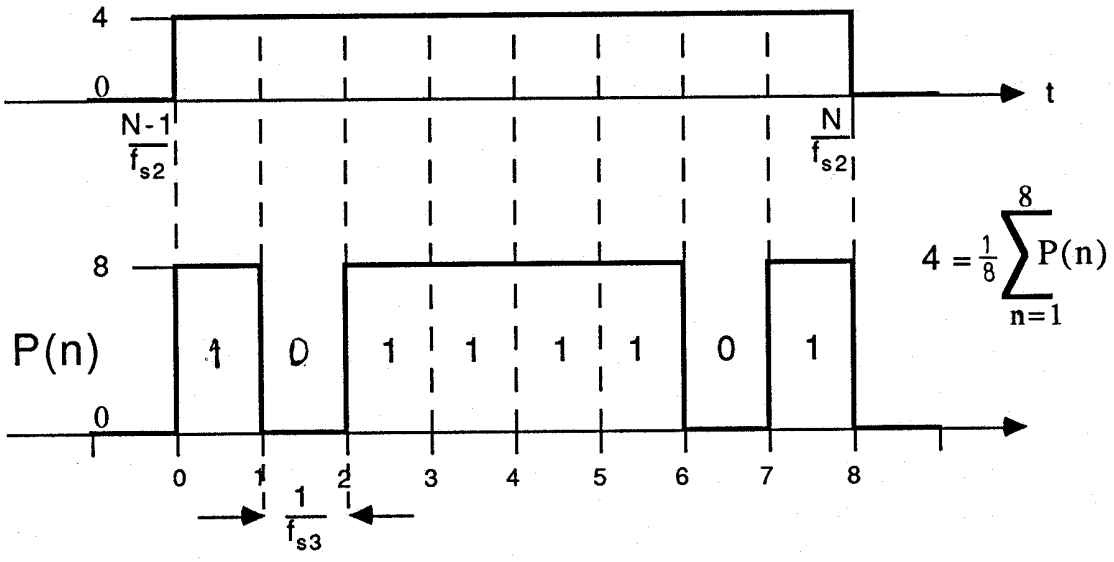

Fig.4 Example code conversion where sequence 10111101 = 4 and code accomodates a maximum level of 8.

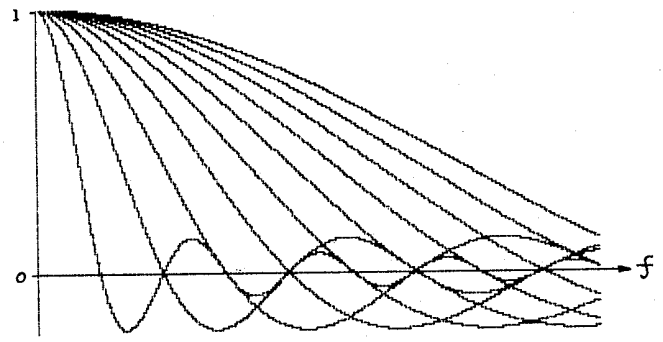

Fig. 5 sin(x)/x frequency response weighting as a function of pulse width : a fundamental distortion mechanism in PWM

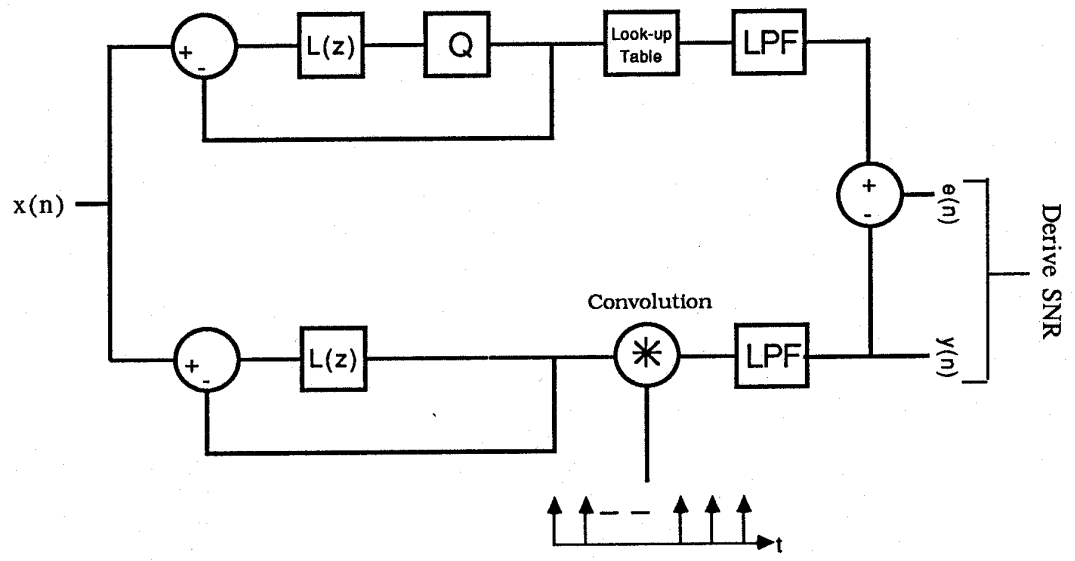

Fig. 6 Computational model for SNR evaluation.

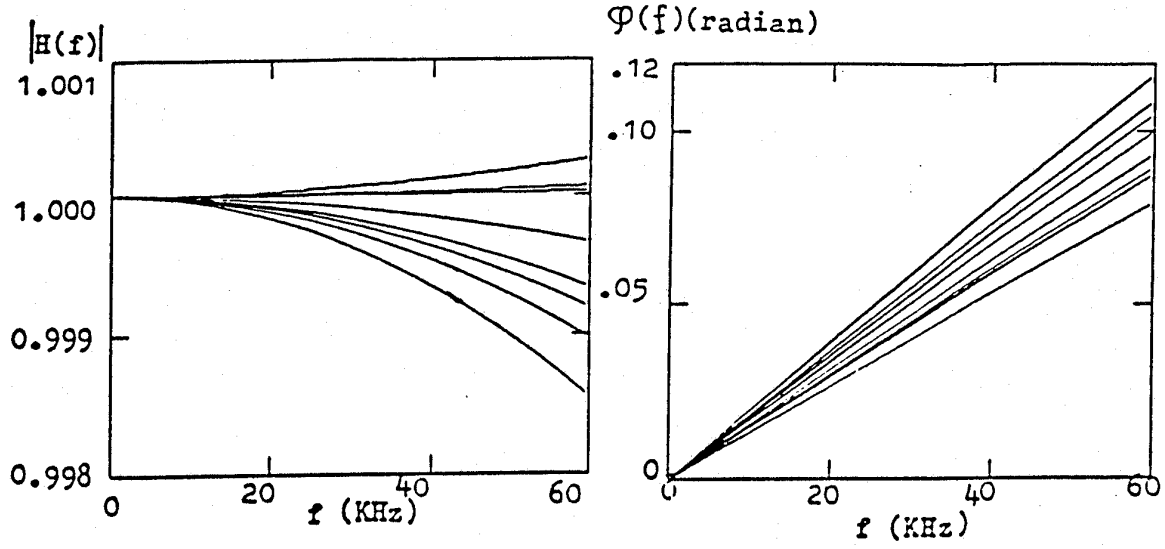

Fig 7a Amplitude and phase plots for coder of Table 1 R=200

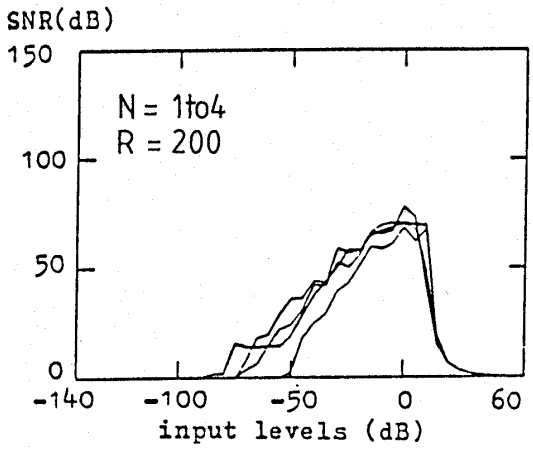

Fig. 7b SNR plots, Table 1

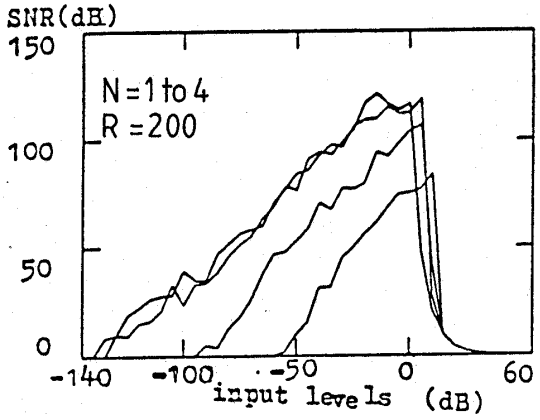

Fig. 8 SNR plots, Table 2

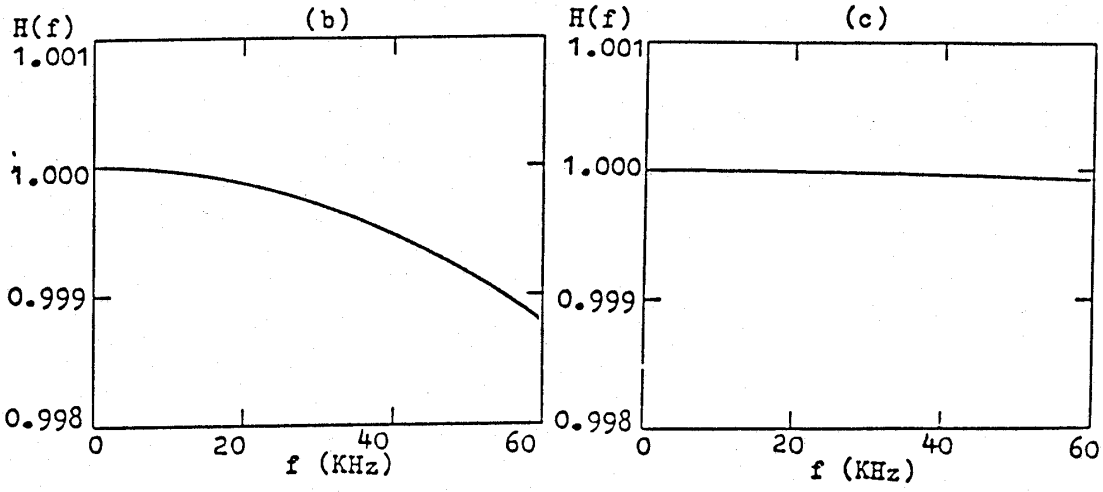

Fig. 9b Transfer function, Table 3, R=50

Fig. 9c Transfer function, Table 3, R = 200

Fig. 9 Spectral plots of coder in Table 3

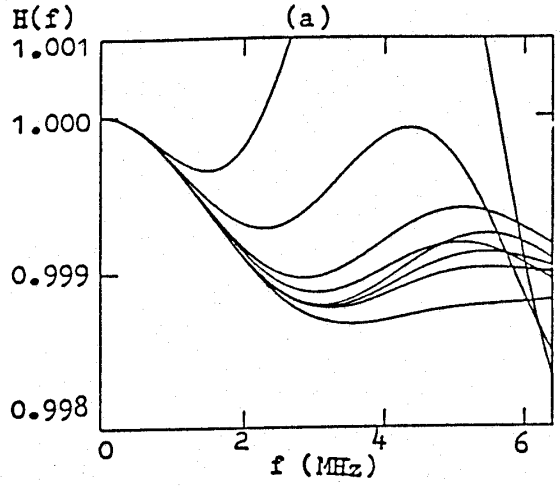

Fig. 9a Table 3 spectral plots of code words, R=200

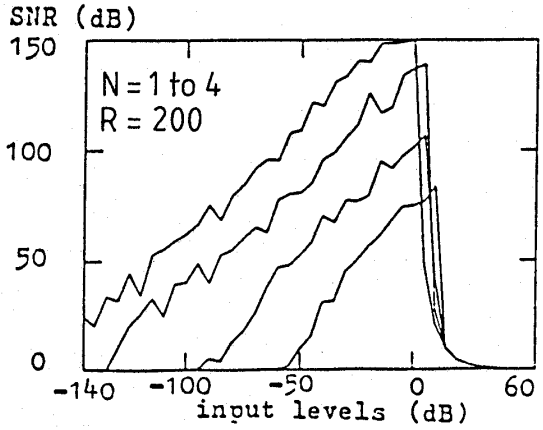

Fig.10 Table 3, SNR plots

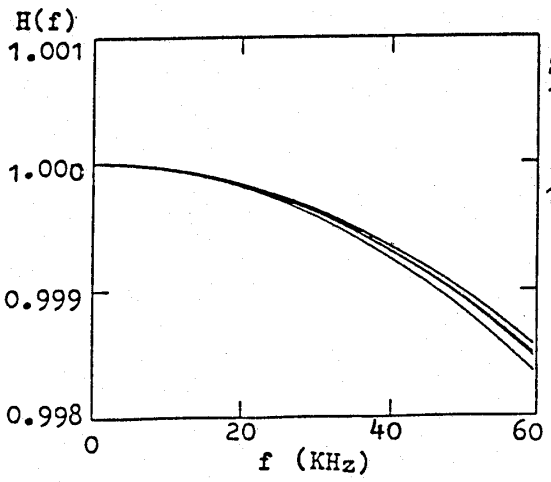

Fig. 11a Transfer function of Table 4, R=200

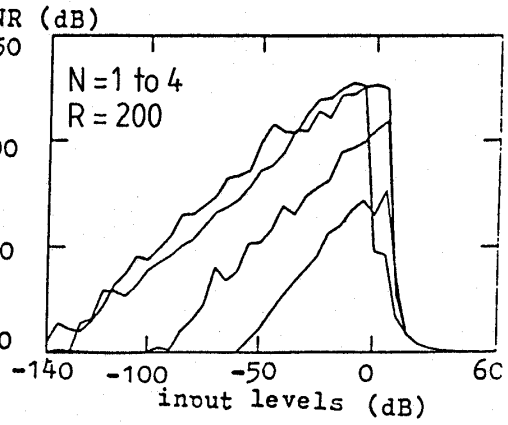

Fig.11b Table 4, SNR plots

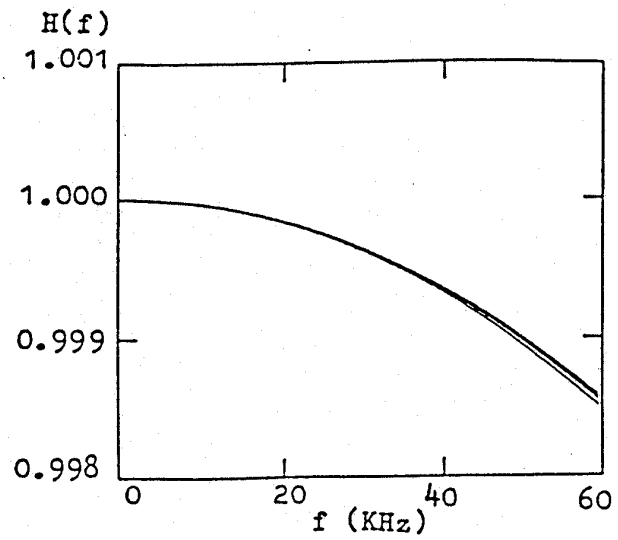

Fig. 12 Transfer function of Table 5

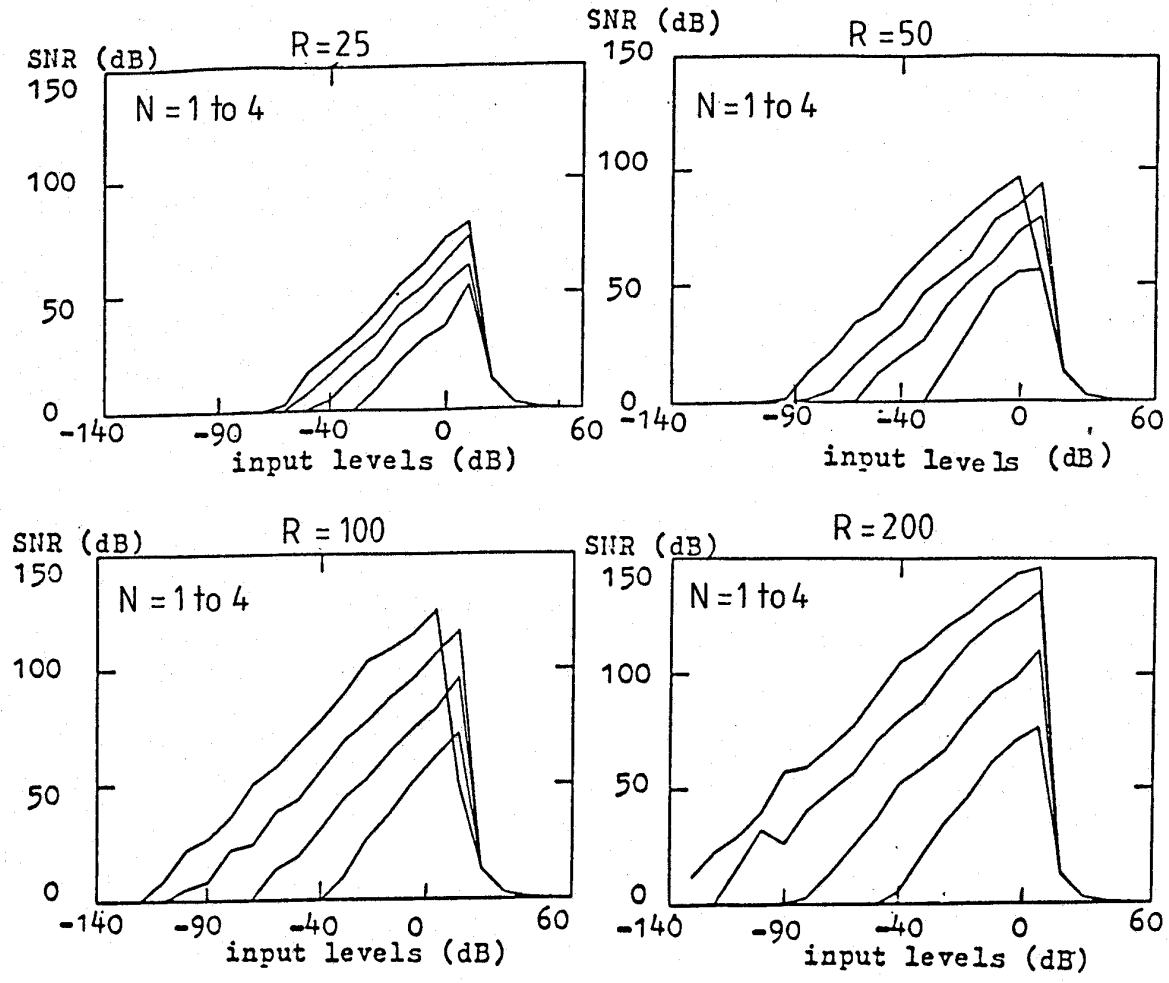

Fig. 13 SNR plots for Table 5